



Effective Lagrangian approach to the EWSB sector

J. Gonzalez–Fraile

Departament d'Estructura i Constituents de la Matèria and ICC-UB, Universitat de Barcelona, 647 Diagonal, E-08028 Barcelona, Spain.

Abstract

In a model independent framework, the effects of new physics at the electroweak scale can be parametrized in terms of an effective Lagrangian expansion. Assuming the $SU(2)_L \times U(1)_Y$ gauge symmetry is linearly realized, the expansion at the lowest order span dimension–six operators built from the observed Standard model (SM) particles, in addition to a light scalar doublet. After a proper choice of the operator basis we present a global fit to all the updated available data related to the electroweak symmetry breaking sector: triple gauge boson vertex (TGV) collider measurements, electroweak precision tests and Higgs searches. In this framework modifications of the interactions of the Higgs field to the electroweak gauge bosons are related to anomalous TGV's, and given the current experimental precision, we show that the analysis of the latest Higgs boson data at the LHC and Tevatron gives rise to strong bounds on TGV's that are complementary to those from direct TGV measurements. Interestingly, we present how this correlated pattern of deviations from the SM predictions could be different for theories based on a non–linear realization of the $SU(2)_L \times U(1)_Y$ symmetry, characteristic of for instance composite Higgs models. Furthermore, anomalous TGV signals expected at first order in the non–linear realization may appear only at higher orders of the linear one, and viceversa. Their study could lead to hints on the nature of the observed boson.

Keywords: Higgs, effective Lagrangian, gauge couplings, LHC

1. Introduction

After the discovery of the Higgs boson [1], we can finally analyze a particle that seems directly related to the electroweak symmetry breaking (EWSB) mechanism. Thus, almost fifty years since the Standard model (SM) Higgs boson was postulated [2], the study of the discovered particle properties can be used for the first time as a way to access the mechanism responsible for the EWSB. In particular, in the present note we focus on the analysis of the Higgs interactions to the rest of SM particles. A huge variety of data has already been collected, not only from Higgs searches at both Tevatron and the LHC, but also from the measurements of triple gauge boson vertices (TGV)'s at the colliders and from the low energy electroweak precision measurements. In

this context we present a framework suitable to study the nature of the observed state via the analysis of its couplings, exploiting all the existing data sets. Pursuing a model independent analysis of the Higgs interactions, the effective Lagrangian approach [3–5] is arguably one of the most motivated frameworks from the theoretical point of view, given the lack of observation of any other new resonance. Hence, the effective Lagrangian is useful as a model independent way to parametrize the low energy deviations in the Higgs interactions caused by New Physics (NP). Following this motivation we present on the first part of this note the effective Lagrangian expansion based on the assumption that the observed state is introduced as a doublet of $SU(2)_L$, where then the $SU(2)_L \otimes U(1)_Y$ symmetry is linearly realized in the effective theory which describes the indirect NP effects at LHC energies [6]. After presenting the results from a global analysis to the different

Email address: fraile@ecm.ub.edu (J. Gonzalez–Fraile)

EWSB related data sets [7, 8], we focus on the very interesting complementarity between Higgs analyses and TGV measurements at colliders [9]. On the second part we compare this phenomenology with the one that is derived from abandoning the assumption of the Higgs as an $SU(2)_L$ doublet. We study in this case the Higgs interactions using the non-linear or chiral effective Lagrangian including a dynamical Higgs boson [10]. We observe that the interesting Higgs to gauge boson coupling correlation with the TGV interactions could be lost in this case, besides higher order differences, that both could lead to phenomenological observable consequences [11] useful to disentangle the nature of the observed state.

2. Lagrangian for an elementary Higgs

We start assuming that, even if there is NP associated with the EWSB sector, the observed particle is an elementary state which belongs to a light electroweak doublet scalar, and consequently, that the $SU(2)_L \otimes U(1)_Y$ symmetry is linearly realized in the effective theory. Thus we think of the SM as an effective low energy theory but we still retain the gauge group, the particle spectrum and the pattern of spontaneous symmetry breaking as valid ingredients to describe Nature at energies $E \ll \Lambda$, where Λ is the scale associated to NP. This fixes the complete set of higher dimensional operators that need to be considered at a given order. Neglecting the effects of the dimension-five total lepton number violating operator, the lowest order effective operators that can be built are of dimension-six:

$$\mathcal{L}_{\text{eff}} = \sum_n \frac{f_n}{\Lambda^2} \mathcal{O}_n, \quad (1)$$

where the operators \mathcal{O}_n have couplings f_n . If we restrict to C and P -even dimension-six operators, 29 of them are relevant to study the Higgs interactions [8] barring flavor structure and Hermitian conjugations. Eight of those modify the Higgs interactions to the electroweak gauge bosons, one to gluons and one affects only Higgs self interactions. Additionally there are three Yukawa-like fermionic operators, and the remaining ones modify both the fermionic couplings to the Higgs boson as well as to the gauge bosons. Finally TGV interactions of on-shell W 's are modified by four of these operators, as well as, by one operator that only involves the electroweak gauge-boson self-couplings, \mathcal{O}_{WWW} , see [9].

Previous to the analysis of the Higgs data the equations of motion can be used to eliminate redundant operators from \mathcal{L}_{eff} . In addition, several operators are already strongly constrained by the use of electroweak

precision data (EWPD), to which they contribute at the tree level. For a detailed discussion on the reduction of the number of parameters in our effective Lagrangian see [8]. After the choice of the basis presented there, the effective Lagrangian relevant for the analysis of Higgs and TGV data, and the subdominant effects to EWPD is reduced to

$$\begin{aligned} \mathcal{L}_{\text{eff}} = & -\frac{\alpha_s v}{8\pi} \frac{f_g}{\Lambda^2} \mathcal{O}_{GG} + \frac{f_{WW}}{\Lambda^2} \mathcal{O}_{WW} + \frac{f_{BB}}{\Lambda^2} \mathcal{O}_{BB} \\ & + \frac{f_{\Phi,2}}{\Lambda^2} \mathcal{O}_{\Phi,2} + \frac{f_{\text{bot}}}{\Lambda^2} \mathcal{O}_{d\Phi,33} + \frac{f_\tau}{\Lambda^2} \mathcal{O}_{e\Phi,33} \quad (2) \\ & + \frac{f_W}{\Lambda^2} \mathcal{O}_W + \frac{f_B}{\Lambda^2} \mathcal{O}_B \end{aligned}$$

with

$$\begin{aligned} \mathcal{O}_{GG} &= \Phi^\dagger \Phi G_{\mu\nu}^a G^{a\mu\nu}, \quad \mathcal{O}_{WW} = \Phi^\dagger \hat{W}_{\mu\nu} \hat{W}^{\mu\nu} \Phi, \\ \mathcal{O}_{BB} &= \Phi^\dagger \hat{B}_{\mu\nu} \hat{B}^{\mu\nu} \Phi, \quad \mathcal{O}_{\Phi,2} = \frac{1}{2} \partial^\mu (\Phi^\dagger \Phi) \partial_\mu (\Phi^\dagger \Phi), \\ \mathcal{O}_{e\Phi,ij} &= (\Phi^\dagger \Phi) (\bar{L}_i \Phi e_{Rj}), \quad \mathcal{O}_{d\Phi,ij} = (\Phi^\dagger \Phi) (\bar{Q}_i \Phi d_{Rj}), \\ \mathcal{O}_W &= (D_\mu \Phi)^\dagger \hat{W}^{\mu\nu} (D_\nu \Phi), \quad \mathcal{O}_B = (D_\mu \Phi)^\dagger \hat{B}^{\mu\nu} (D_\nu \Phi), \quad (3) \end{aligned}$$

where Φ is the Higgs doublet, $D_\mu \Phi = (\partial_\mu + i\frac{1}{2}g'B_\mu + ig\frac{\sigma_a}{2}W_\mu^a)\Phi$ and v is the vacuum expectation value. $\hat{B}_{\mu\nu} = i\frac{g'}{2}B_{\mu\nu}$ and $\hat{W}_{\mu\nu} = i\frac{g}{2}\sigma^a W_{\mu\nu}^a$, with $SU(2)_L$ ($U(1)_Y$) gauge coupling g (g') and Pauli matrices σ^a .

The dimension-six operators in the final basis to be studied, Eq. (2), contribute to the interactions of the Higgs boson with the SM particles, in some cases adding new Lorentz structures in the different vertices, as it was discussed in detail in [8]. In addition, two of them, \mathcal{O}_W and \mathcal{O}_B , contribute to the TGV interactions $\gamma W^+ W^-$ and $Z W^+ W^-$, whose contributions in the commonly used parametrization of [12] are:

$$\begin{aligned} \Delta\kappa_\gamma &= \frac{g^2 v^2}{8\Lambda^2} (f_W + f_B), \\ \Delta g_1^Z &= \frac{g^2 v^2}{8c^2 \Lambda^2} f_W, \quad \Delta\kappa_Z = \frac{g^2 v^2}{8c^2 \Lambda^2} (c^2 f_W - s^2 f_B), \quad (4) \end{aligned}$$

with $\kappa_V = 1 + \Delta\kappa_V$ and $g_1^Z = 1 + \Delta g_1^Z$, and where $s(c)$ is the sine (cosine) of the weak mixing angle. For completeness we note that \mathcal{O}_{WWW} contributes to the TGV parametrization in [12] as $\lambda_\gamma = \lambda_Z = \frac{3g^2 M_W^2}{2\Lambda^2} f_{WWW}$, although it has no relevance for the present note. Finally, \mathcal{O}_W , \mathcal{O}_B , \mathcal{O}_{WW} , \mathcal{O}_{BB} and $\mathcal{O}_{\Phi,2}$ also give subdominant (loop) contributions to EWPD.

In order to constrain these higher dimensional deviations with respect to the Standard Model expected behaviour we build a χ^2 function based on the signal

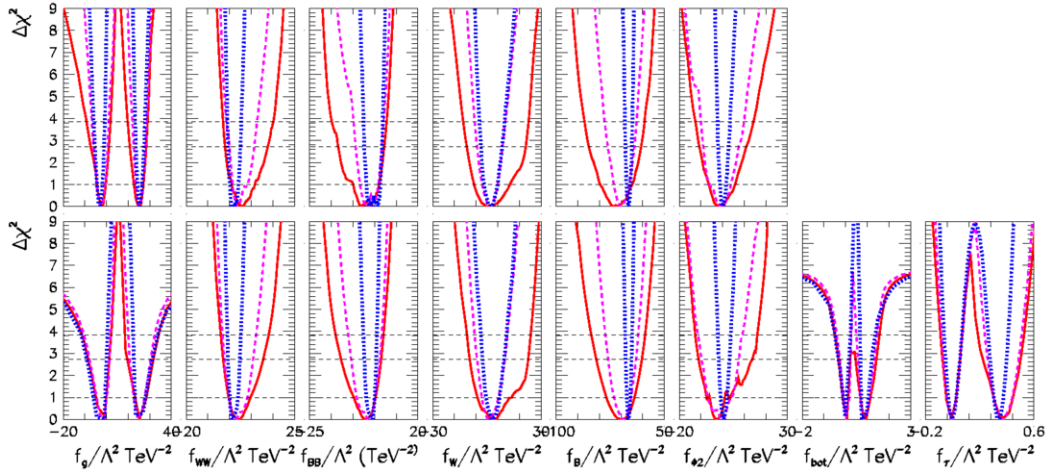


Figure 1: $\Delta\chi^2$ dependence on the fit parameters when we consider all Higgs collider data (red solid lines), Higgs collider plus TGV data (dashed purple lines), and Higgs collider plus TGV and EWP data (dotted blue lines). The columns depict the $\Delta\chi^2$ dependence with respect to the fit parameter shown in the bottom, with the anomalous couplings f/Λ^2 given in TeV^{-2} , while the rest of undisplayed parameters are marginalized. In the upper row we use $f_g, f_{WW}, f_{BB}, f_W, f_B,$ and $f_{\phi,2}$ as fit parameters with $f_{\text{bot}} = f_\tau = 0$, while in the bottom row the fitting parameters are $f_g, f_{WW} = -f_{BB}, f_W, f_B, f_{\phi,2}, f_{\text{bot}}$ and f_τ .

strength measurements of the Higgs production and decay at both the Tevatron and LHC, together with the addition of the most precise determination of TGV's at the colliders in the present framework, as well as the inclusion of EWP data in a simplified way in terms of the oblique parameters S, T and U . The details on the data included on this global analysis, as well as the statistical details of the fit are described thoroughly in [7, 8].

2.1. Results

In order to study the present bounds on the Higgs interactions from Higgs, TGV and EWP data sets we perform several global analyses including different data and dimension–six operator sets. The results are shown in Fig. 1.

In the Figure one can see the $\Delta\chi^2$ dependence on the fit parameters when we consider all Higgs collider data (red solid lines), Higgs collider plus TGV data (dashed purple lines), and Higgs collider plus TGV and EWP data (dotted blue lines). In the columns we show the $\Delta\chi^2$ dependence with respect to the fit parameter written in the bottom of the column, with f/Λ^2 given in TeV^{-2} , and while the rest of undisplayed parameters have been marginalized. In the upper row we use $f_g, f_{WW}, f_{BB}, f_W, f_B,$ and $f_{\phi,2}$ as fit parameters with $f_{\text{bot}} = f_\tau = 0$, while in the bottom row the fitting parameters are $f_g, f_{WW} = -f_{BB}, f_W, f_B, f_{\phi,2}, f_{\text{bot}}$ and f_τ . With the precision

reachable from the considered data sets the main conclusion that we can extract is that so far all the considered Higgs and gauge interactions are completely compatible with the SM Higgs hypothesis. This causes all the $\Delta\chi^2$ panels to have the minima close to the 0 point (SM point) without any statistically significant deviation with respect to the SM pattern of interactions. The degeneracies in f_g, f_{bot} and f_τ are due to the interference with the SM corresponding vertices. In addition, by comparing the results for the upper and lower operator sets considered, we can observe that the introduction of the fermionic operators to the analysis has a negligible effect on O_W, O_B, O_{WW}, O_{BB} and $O_{\phi,2}$. An exception is the observed weakening of the exclusion ranges on f_g , which is strongly related to the inclusion of f_{bot} , as discussed in [8]. Fig. 1 is useful to illustrate some of the interesting features and the potential of the data–driven approach, as it allows us to identify which of the data sets impose the strongest constraints on a given operator. For instance, by looking at either the f_W or f_B panels, either the upper or the lower row, we could already foresee comparing the results from the analysis of the Higgs data to the results from the combined analysis of Higgs and TGV data that the precision reachable from both data sets on f_W or f_B is at a similar level. A conclusion that drives us directly to the following subsection.

2.2. Determining TGV from Higgs data

As we have commented, two of the operators, O_W and O_B , contribute both to the Higgs interactions with the gauge bosons, and to TGV interactions. In the results presented in Fig. 1 we have used this double contribution on the direction of adding TGV data to the global analysis of the dimension–six operators in order to further constrain the coefficients of the operators considered in Eq. (2). Conversely, we can exploit this double contribution on qualitatively the opposite direction. We present now the global analysis of only Higgs data, but this time we rotate the exclusion bounds derived from the results to bounds on the TGV parameters by using Eq. (4). As we have observed in the previous subsection that the fermionic operators do not affect the electroweak ones, for simplicity we show in this subsection the results of the space spanned by $f_g, f_{WW}, f_{BB}, f_{\Phi,2}, f_W$, and f_B . We present the results of the analysis to the Higgs data only in Fig. 2. There we plot in the red filled region the 95% C.L. allowed values in the plane $\Delta\kappa_\gamma \otimes \Delta g_1^Z$ after marginalizing over the other four parameters on the Higgs analysis, f_g, f_{WW}, f_{BB} and $f_{\Phi,2}$, *i.e.* we define

$$\Delta\chi_H^2(\Delta\kappa_\gamma, \Delta g_1^Z) = \min_{f_g, f_{WW}, f_{BB}, f_{\Phi,2}} \Delta\chi_H^2(f_g, f_{WW}, f_{BB}, f_{\Phi,2}, f_B, f_W) , \quad (5)$$

and we impose the two-dimensional 95% C.L. allowed region from the condition $\Delta\chi_H^2(\Delta\kappa_\gamma, \Delta g_1^Z) \leq 5.99$. In the Figure we also show the relevant 95% C.L. bounds from TGV measurements in different collider experiments as properly labeled. These experimental measurements were all performed in the framework given by Eq. (4), for further details see [9]. As we can observe in the Figure, the direct measurements of TGV’s and the results derived from the global analysis of Higgs data translated to the TGV space, are not only complementary because of the different correlation that they present, but actually the precision reachable from both types of determinations are at a comparable level. As a consequence, this interesting complementarity between both analysis can be used as a further test of the SM and of the linearly realized EWSB. In the future, when the data sets are extended, the combination of both types of analysis has the potential to furnish the strongest possible bounds on this anomalous TGV space. Indeed, after performing the current combination of results, as described in [9], the hatched region in Fig. 2 sets the strongest 95% C.L. exclusion region of the ones currently available.

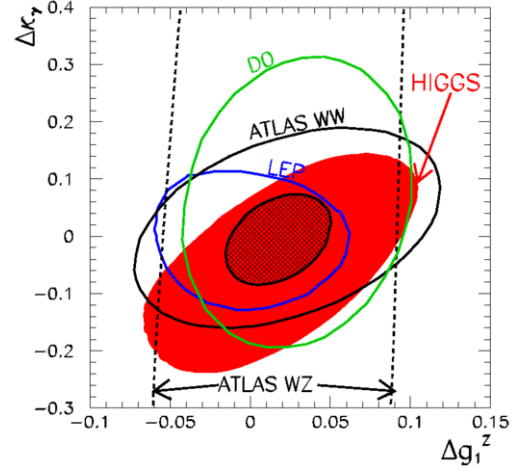


Figure 2: 95% C.L. allowed regions (2 d.o.f.) on the plane $\Delta\kappa_\gamma \otimes \Delta g_1^Z$ from the global analysis of only Higgs data from the LHC and Tevatron (red filled region), and relevant bounds from TGV measurements in different collider experiments as labeled in the panel. We also show the estimated constraints obtainable by combining these bounds (hatched region).

3. Disentangling a dynamical Higgs

We proceed now to compare the phenomenology of the effective Lagrangian expansion assuming a linear realization of the EWSB with the phenomenology of the non–linear or chiral Lagrangian expansion, including a light Higgs, but in this case generically as a singlet of $SU(2)_L$. While the first expansion is suitable for models with elementary Higgs particles, the second one may be more adequate for “dynamical” –composite– ones. For the non–linear case we consider the construction of the effective Lagrangian presented in [10], up to four derivatives in the expansion and including the bosonic and Yukawa–like C and P even operators¹. For the comparison of the phenomenology, we can start restricting to the subset of chiral operators that include the same gauge interactions that are already introduced by the dimension–six operators in the linear expansion, *i.e.* we consider the chiral structures weighted by the parameter ξ in [10, 11]. The lesser symmetry constraints in the non–linear effective Lagrangian means more possible invariant operators at a given order, which is translated into phenomenological decorrelations with respect to the linear case, differences that we present here. For

¹With an increased precision some of these assumptions may be relaxed, allowing for instance for C and P violating operators to be included and studied [13].

instance, in the unitary gauge, two of the non-linear operators, $\mathcal{P}_2(h)$ and $\mathcal{P}_4(h)$ in the notation of [11], read:

$$\mathcal{P}_2(h) = 2ie g^2 A_{\mu\nu} W^{-\mu} W^{+\nu} \mathcal{F}_2(h) - 2 \frac{ie^2 g}{\cos \theta_W} Z_{\mu\nu} W^{-\mu} W^{+\nu} \mathcal{F}_2(h), \quad (6)$$

$$\mathcal{P}_4(h) = -\frac{eg}{\cos \theta_W} A_{\mu\nu} Z^\mu \partial^\nu \mathcal{F}_4(h) + \frac{e^2}{\cos^2 \theta_W} Z_{\mu\nu} Z^\mu \partial^\nu \mathcal{F}_4(h), \quad (7)$$

with their coefficients c_2 and c_4 taking arbitrary (model dependent) values, and where the model dependent functions $\mathcal{F}(h)$ encode the chiral interactions of the light h . In contrast, the $d = 6$ operator containing the same gauge interactions, O_B , results in the combination:

$$O_B = \frac{ieg^2}{8} A_{\mu\nu} W^{-\mu} W^{+\nu} (v+h)^2 - \frac{ie^2 g}{8 \cos \theta_W} Z_{\mu\nu} W^{-\mu} W^{+\nu} (v+h)^2 \quad (8)$$

$$- \frac{eg}{4 \cos \theta_W} A_{\mu\nu} Z^\mu \partial^\nu h (v+h) + \frac{e^2}{4 \cos^2 \theta_W} Z_{\mu\nu} Z^\mu \partial^\nu h (v+h). \quad (9)$$

In consequence, in a general non-linear analysis the γWW interactions get decorrelated from the γZh and ZZh couplings, all encoded in O_B , and for the precise Lorentz structures shown above. These interactions construct in the linear case the correlation that leads to the interesting complementarity between Higgs data analysis and the direct measurement of TGV's that we have highlighted in the previous section when exploiting the effective Lagrangian analysis in the linear realization of the EWSB. Thus in order to study whether the EWSB mechanism presents a correlated or a decorrelated behaviour, we can perform the global analysis of Higgs, TGV and EWPD in the context of the non-linear effective Lagrangian, what is the first 8-dimensional analysis in this basis [11]. While the complete details of such study can be found in [11], here we only show a subset of the two-dimensional results. But instead of showing the ranges of results as a function of the coefficients of the non-linear operators included in the global analysis, we rotate part of the coefficients to a new set of variables, see [11]. This is illustrated in Fig. 3, where the results of the combined analysis of the data sets considered have been projected into combinations of the non-linear operators $\mathcal{P}_2(h)$, $\mathcal{P}_3(h)$, $\mathcal{P}_4(h)$ and $\mathcal{P}_5(h)$:

$$\Sigma_B \equiv 4(2c_2 + a_4), \quad \Sigma_W \equiv 2(2c_3 - a_5), \quad (10)$$

$$\Delta_B \equiv 4(2c_2 - a_4), \quad \Delta_W \equiv 2(2c_3 + a_5), \quad (11)$$

defined such that at order $d = 6$ of the linear expansion $\Sigma_B = f_B$, $\Sigma_W = f_W$, while $\Delta_B = \Delta_W = 0$. In the expressions c_i and a_i stand for the relevant coefficients of the non-linear operators considered for the comparison [11], where in the non-linear case we have included the light Higgs in the generic functions in Eqs. (6) and (7), assuming $\mathcal{F}_i(h) \equiv 1 + 2\tilde{a}_i \frac{h}{v} + \dots$, where the dots stand for higher powers of h/v that are irrelevant for the present note, and where to further simplify the notation

$a_i \equiv c_i \tilde{a}_i$, with c_i being the global chiral operator coefficients. With these variables, the (0,0) coordinate corresponds to the SM in the upper figure of Fig. 3, while in the lower figure it corresponds to the linear regime (at order $d = 6$). Would future data point to a departure from (0,0) in the variables of the first figure it would indicate BSM physics irrespective of the linear or non-linear character of the underlying dynamics; while such a departure in the bottom one would be consistent with a non-linear realization of EWSB.

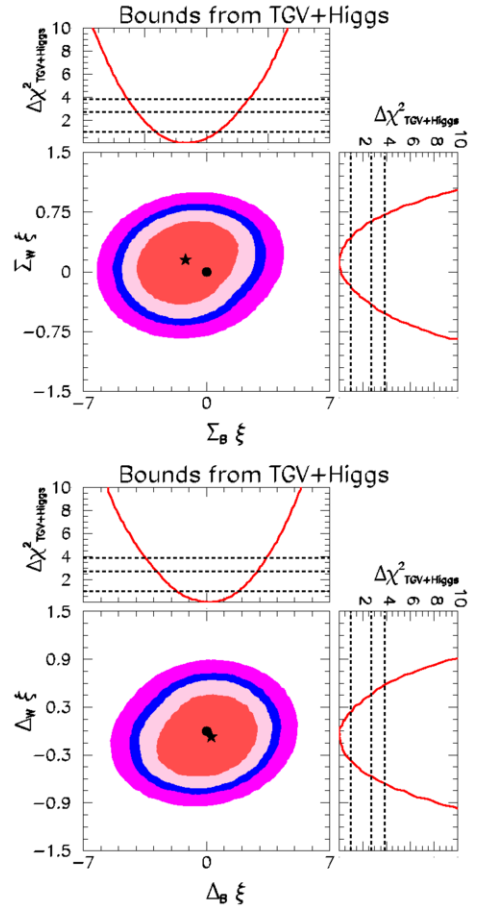


Figure 3: **Upper:** A BSM sensor irrespective of the type of expansion: constraints from TGV and Higgs data on the combinations $\Sigma_B = 4(2c_2 + a_4)$ and $\Sigma_W = 2(2c_3 - a_5)$, which converge to f_B and f_W in the linear $d = 6$ limit. The dot at (0,0) signals the SM expectation. **Lower:** A non-linear versus linear discriminator: constraints on the combinations $\Delta_B = 4(2c_2 - a_4)$ and $\Delta_W = 2(2c_3 + a_5)$, which would take zero values in the linear (order $d = 6$) limit (as well as in the SM), indicated by the dot at (0,0). For both figures the lower left panels shows the 2-dimensional allowed regions at 68%, 90%, 95%, and 99% CL after marginalization with respect to the rest of parameters spanned in the analysis, see [11]. The star corresponds to the best fit point of the analysis. The upper left and lower right panels in each figure give the corresponding 1-dimensional projections over each of the two combinations considered.

Additional phenomenological differences between both effective Lagrangian expansions were further studied in [11]. They involve interactions that may be generated by leading operators in one of the expansions, while they can only be generated by subleading– and then suppressed– operators in the alternative approach. Several examples of this type of higher order differences, as well as a realistic analysis of the LHC capability to improve the precision on some of the interactions involved can be found in [11]. They require a more detailed analysis of anomalous TGV's.

4. Conclusions

In this note we have presented some of the interesting features of the model independent analysis of the Higgs interactions by means of an effective Lagrangian expansion. In the first part we have presented a global analysis of Higgs, TGV and EWPD assuming that the Higgs is part of an $SU(2)_L$, and thus that the EWSB is linearly realized. From this analysis in terms of dimension–six operators we have concluded that currently the considered Higgs couplings to the SM particles as well as the studied gauge self–interactions are completely compatible with the SM Higgs hypothesis within the reachable precision. With the data–driven approach that we have followed we have been able to identify a very interesting complementarity between the direct measurement at the colliders of the TGV interactions and the results obtained from a global analysis of the Higgs data. The combination of both types of analysis has the potential to lead to the strongest sensitivity on deviations from the SM pattern of interactions in the TGV's, being useful as a consequence to further test the SM and the linearly realized EWSB. Interestingly we have illustrated that this correlated pattern of interactions may disappear when we consider an alternative expansion, the non–linear effective Lagrangian. In this case the lesser symmetry constraints could be translated in general scenarios in the decorrelation between Higgs to gauge bosons and TGV interactions. We have presented a possible set of variables to study how the collected data allow us to disentangle the two possible expansions, and as a consequence the nature of the observed state and EWSB mechanism.

The contents of this note are based on the published works [7–9, 11], the author thanks his collaborators in these studies. J.G-F acknowledges support from European Union network FP7 ITN INVISIBLES (Marie Curie Actions, PITN-GA-2011-289442), MICINN FPA2010-20807, consolidator-ingenio 2010

program CSD-2008-0037 and ME FPU grant AP2009-2546.

References

- [1] S. Chatrchyan *et al.* [CMS Collaboration], “Observation of a new boson at a mass of 125 GeV with the CMS experiment at the LHC,” *Phys. Lett. B* **716** (2012) 30 [arXiv:1207.7235 [hep-ex]]. G. Aad *et al.* [ATLAS Collaboration], “Observation of a new particle in the search for the Standard Model Higgs boson with the ATLAS detector at the LHC,” *Phys. Lett. B* **716** (2012) 1 [arXiv:1207.7214 [hep-ex]].
- [2] F. Englert and R. Brout, *Phys.Rev.Lett.* **13**, 321 (1964). P. W. Higgs, *Phys.Rev.Lett.* **13**, 508 (1964). P. W. Higgs, *Phys.Lett.* **12**, 132 (1964). G. Guralnik, C. Hagen, and T. Kibble, *Phys.Rev.Lett.* **13**, 585 (1964). P. W. Higgs, *Phys.Rev.* **145**, 1156 (1966). T. Kibble, *Phys.Rev.* **155**, 1554 (1967).
- [3] S. Weinberg, *Physica* **96A**, 327 (1979);
- [4] H. Georgi, *Weak Interactions and Modern Particle Theory* (Benjamin/Cummings, Menlo Park, 1984)
- [5] J. F. Donoghue, E. Golowich and B. R. Holstein, *Dynamics of the Standard Model* (Cambridge University Press, 1992).
- [6] W. Buchmuller and D. Wyler, *Nucl. Phys.* **B268**, 621 (1986); C. N. Leung, S. Love, and S. Rao, *Z. Phys.* **C31**, 433 (1986); B. Grzadkowski, M. Iskrzynski, M. Misiak and J. Rosiek, *JHEP* **1010**, 085 (2010) [arXiv:1008.4884 [hep-ph]]. A. De Rijula, M. Gavela, P. Hernandez, and E. Masso, *Nucl. Phys.* **B384**, 3 (1992). K. Hagiwara, S. Ishihara, R. Szalapski, and D. Zeppenfeld, *Phys. Rev.* **D48**, 2182 (1993); K. Hagiwara, R. Szalapski, and D. Zeppenfeld, *Phys. Lett.* **B318**, 155 (1993) [arXiv:hep-ph/9308347]; K. Hagiwara, S. Matsumoto, and R. Szalapski, *Phys. Lett.* **B357**, 411 (1995) [arXiv:hep-ph/9505322]. K. Hagiwara, T. Hatsukano, S. Ishihara and R. Szalapski, *Nucl. Phys. B* **496**, 66 (1997) [hep-ph/9612268]. M. Gonzalez-Garcia, *Int. J. Mod. Phys.* **A14**, 3121 (1999), arXiv:hep-ph/9902321; F. de Campos, M. C. Gonzalez-Garcia and S. F. Novaes, *Phys. Rev. Lett.* **79**, 5210 (1997) [hep-ph/9707511]; M. C. Gonzalez-Garcia, S. M. Lietti and S. F. Novaes, *Phys. Rev. D* **57**, 7045 (1998) [hep-ph/9711446]; O. J. P. Eboli, M. C. Gonzalez-Garcia, S. M. Lietti and S. F. Novaes, *Phys. Lett. B* **434**, 340 (1998) [hep-ph/9802408]; M. C. Gonzalez-Garcia, S. M. Lietti and S. F. Novaes, *Phys. Rev. D* **59**, 075008 (1999) [hep-ph/9811373]; O. J. P. Eboli, M. C. Gonzalez-Garcia, S. M. Lietti and S. F. Novaes, *Phys. Lett. B* **478**, 199 (2000) [hep-ph/0001030]. G. Passarino, *Nucl. Phys. B* **868**, 416 (2013) [arXiv:1209.5538 [hep-ph]].
- [7] T. Corbett, O. J. P. Eboli, J. Gonzalez-Fraile and M. C. Gonzalez-Garcia, *Phys. Rev. D* **86**, 075013 (2012) [arXiv:1207.1344 [hep-ph]].
- [8] T. Corbett, O. J. P. Eboli, J. Gonzalez-Fraile and M. C. Gonzalez-Garcia, *Phys. Rev. D* **87**, 015022 (2013) [arXiv:1211.4580 [hep-ph]].
- [9] T. Corbett, O. J. P. Eboli, J. Gonzalez-Fraile and M. C. Gonzalez-Garcia, *Phys. Rev. Lett.* **111**, 011801 (2013) [arXiv:1304.1151 [hep-ph]].
- [10] R. Alonso, M. B. Gavela, L. Merlo, S. Rigolin and J. Yepes, *Phys. Lett. B* **722**, 330 (2013) [Erratum-ibid. *B* **726**, 926 (2013)] [arXiv:1212.3305 [hep-ph]].
- [11] I. Brivio, T. Corbett, O. J. P. Eboli, M. B. Gavela, J. Gonzalez-Fraile, M. C. Gonzalez-Garcia, L. Merlo and S. Rigolin, *JHEP* **1403**, 024 (2014) [arXiv:1311.1823 [hep-ph]].
- [12] K. Hagiwara, R. Peccei, D. Zeppenfeld, and K. Hikasa, *Nucl. Phys.* **B282**, 253 (1987).
- [13] M. B. Gavela, J. Gonzalez-Fraile, M. C. Gonzalez-Garcia, L. Merlo, S. Rigolin and J. Yepes, [arXiv:1406.6367 [hep-ph]].